Chemistry & Biology, Vol. 10, 759–767, August, 2003, ©2003 Elsevier Science Ltd. All rights reserved. DOI 10.1016/S1074-5521(03)00157-1

Development and Characterization of Nonpeptidic Small Molecule Inhibitors of the XIAP/Caspase-3 Interaction

Tom Y.H. Wu,[1] Klaus W. Wagner,[2] Badry Bursulaya,[2] Peter G. Schultz,[1,2,*] and Quinn L. Deveraux[2,*]

[1]The Scripps Research Institute
10550 North Torrey Pines Road
La Jolla, California 92037

[2]Genomics Institute
of the Novartis Research Foundation
10675 John Jay Hopkins Drive
San Diego, California 92121

Summary

Elevated expression of inhibitor of apoptosis protein (IAP) family members in various types of cancers is thought to provide a survival advantage to these cells. Thus, antiapoptotic functions of IAPs, and their potential as novel anticancer targets have attracted considerable interest. Among the IAPs, the X chromosome-linked inhibitor of apoptosis protein (XIAP) is regarded as the most potent suppressor of mammalian apoptosis through direct binding and inhibition of caspases. A high-throughput biochemical screen of a combinatorial chemical library led to the discovery of a novel nonpeptidic small molecule that has the ability to disrupt the XIAP/caspase-3 interaction. The activity of this nonpeptidic small molecule inhibitor of the XIAP/caspase-3 interaction has been characterized both in vitro and in cells. Molecules of this type can be used to conditionally inhibit the cellular function of XIAP and may provide insights into the development of therapeutic agents that act by modulating apoptotic pathways.

Introduction

The ability to evade cell death through suppression of apoptosis is considered one of the essential hallmarks of human cancers [1]. Apoptosis pathways in mammalian cells are divided into two categories: extrinsic and intrinsic. While the extrinsic pathway is activated by cellular death receptor-ligand interactions, the intrinsic pathway is regulated through the mitochondria. Both pathways ultimately activate effector caspases (cysteinyl aspartate-specific proteases), mainly caspase-3 and -7 to induce apoptosis [2–4]. Suppression of these effector caspases by misregulation of both pro- and antiapoptotic proteins provides a survival advantage during oncogenesis and facilitates resistance to chemotherapies. Among the antiapoptotic proteins that have been implicated in this process is the inhibitor of apoptosis protein (IAP) family [2–4]. Characterization of antiapoptotic proteins, including IAPs, has resulted in the development of new strategies targeting cancer survival mechanisms, some of which are now being tested in clinical trials for cancer treatment [5].

Among the IAP family members, the X chromosome-linked inhibitor of apoptosis protein (XIAP) is regarded as the most potent suppressor of cell death [6]. XIAP consists of four major domains: BIR1, BIR2, BIR3, and RING. At least one explanation for the versatile suppression of cell death exhibited by XIAP resides in its ability to inhibit caspases [3, 4]. More specifically, the BIR1-2 region of XIAP is a potent and specific inhibitor of caspases-3 and -7, whereas BIR3 is specific for caspase-9 [7–9, 10]. Besides inhibiting caspases, XIAP has been reported to induce cell-cycle arrest and active signal transduction pathways mediated by NFκB, c-Jun amino-terminal kinase, and SMAD-dependent transcription [3].

Posttranslationally, XIAP can be regulated by inhibitory proteins, such as Smac (second mitochondrial activator of caspases) [11]. Following appropriate apoptotic stimuli, Smac is released from the mitochondria to disrupt XIAP-caspase complexes. Caspases, once liberated from XIAP inhibition, execute apoptosis by the specific proteolysis of a wide variety of substrates ultimately leading to cell death. The molecular details of the Smac-XIAP interaction have recently been revealed by the X-ray cocrystal structures of the XIAP-BIR3 region in complex with Smac-derived peptides [12, 13]. These structures, in combination with a recent report describing the mechanisms of caspase-9 activation, have provided insights into the mechanism by which Smac blocks BIR3-mediated inhibition of caspase-9 [14]. However, similar structural studies addressing the role of full-length Smac in the relief of XIAP-BIR1-2-mediated inhibition of caspases-3 and -7 have yet to be described [7–9]. Smac-derived peptides have been reported to bind the caspase-9 binding site on XIAP-BIR3 [15]; they have also been shown to facilitate activation of procaspase-3 [16], although it is unclear if this results from direct inhibition of XIAP binding to active caspase-3.

Since both the extrinsic and intrinsic apoptosis pathways require the executioner caspase-3, molecular tools that modulate the interaction of caspase-3/XIAP should be useful probes of the cellular functions of these proteins. Such molecules could ultimately lead to anticancer therapies. Here, we describe the identification of a nonpeptidic small molecule inhibitor of the caspase-3/XIAP interaction from a combinatorial chemical library using high-throughput screening. Furthermore, this inhibitor was used to probe the function of XIAP in relevant biochemical and cell-based tumor models.

Discovery and Synthesis of Small Molecule Inhibitors of XIAP/Caspase-3

Since active caspase-3 is efficiently inhibited by XIAP, the enzymatic activity of caspase-3 was used to screen for inhibitors of the XIAP/caspase-3 interaction (Figure 1A). Recombinant XIAP was incubated with compounds in buffer containing fluorogenic caspase-3 substrate (Ac-DEVD-afc), followed by caspase-3 addition. Mole-

*Correspondence: deveraux@gnf.org (Q.L.D.), schutlz@gnf.org (P.G.S.)

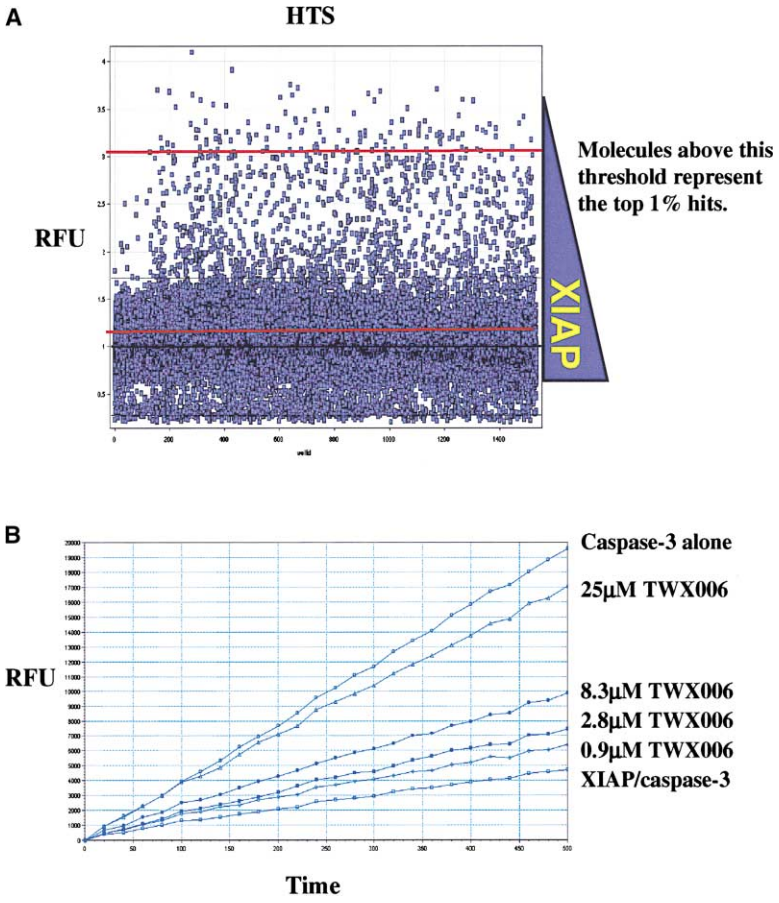

Figure 1. XIAP/Caspase-3 Activity Assay

(A) Small molecules were coincubated with caspase-3 and XIAP in a high-throughput screening (HTS) format, and fluorescence intensities were plotted on a graph for each of the compound tested. The fluorescence intensity inversely correlates with inhibition of XIAP on caspase-3.

(B) Caspase-3 alone causes an increase in fluorescence over time as the Ac-DEVD-afc substrates are being hydrolyzed. Coincubation with XIAP decreases the fluorescence intensity due to caspase-3 inhibition. As an example, addition of TWX006 at 1, 3, 9, and 25 μM concentration resulted in a dose-dependent increase in fluorescence signal.

cules that block XIAP/caspase-3 complex formation are expected to restore caspase activity, which is measured by cleavage of the fluorogenic peptide substrate (Figure 1B) [17]. Screening a library containing approximately 160,000 compounds in a 1536-well format identified several moderately active small molecules. Control assays confirmed that these molecules do not influence caspase-3 activity in the absence of XIAP (data not shown). In addition, it was observed that longer preincubation of compounds with XIAP resulted in faster activation of caspase relative to preincubation with caspase-3, suggesting that these molecules may bind to XIAP instead of caspase-3. Unfortunately, the inhibitors identified from the primary screen exhibited poor solubility in aqueous solution. At 20 μM concentration in aqueous media, most active small molecules precipitated overnight; therefore, their usefulness in cell models is limited. Hence, a small focused library of molecules (named TWX) based on the original hits was synthesized with the aim of finding XIAP inhibitors with improved physical properties and/or affinity, which are more suitable for studies in cellular systems.

The TWX molecular scaffold can be broken down into four fragments, each of which can be substituted by a series of diverse building blocks with solid-phase organic synthesis (Figure 2A). The first fragment (Figures 2B, 1-A to 1-D), which can be substituted by any of a series of diamine linkers, is incorporated by condensation of the amine in N,N-dimethylformamide (DMF) at room temperature with a polystyrene carbamate resin [18]. The initial loading of the resin is approximately 1.0 mmol/g. The second fragment (Figure 2B, 2-A to 2-P) can be substituted with a variety of aryl sulfonyl and carbonyl chlorides and is introduced by a condensation reaction with quantitative conversion. Depending on the nature of the aryl substituents, the third building block, which again is chosen from diamine linkers (Figure 2B, 3-A to 3-E), can be introduced by two different strategies. If the aryl substituent X is the more electron-withdrawing fluorine, the diamine can be incorporated by a S_NAr reaction by heating the starting resin in N-methylpyrrolidine (NMP) at 80°C in the presence of the diamine for 24 hr. This reaction is complicated by the dimerization of the molecule on solid support, as one diamine molecule contains two nucleophilic ends. Nevertheless, by using large excess of the diamine (20 equivalents), dimerized side product is reduced to less than 15%. If X is bromine or iodine, a palladium cross-coupling method was used with $Pd_2(dba)_3$ as the catalyst and 2-(di-*tert*-butylphosphino)biphenyl as the ligand in the presence of potassium *tert*-butoxide in DMF at 80°C [19]. Again, the dimerization problem was suppressed by adding excess diamine, and the yields of the desired product were typically in the range of 75%–90%. The fourth fragment consisted of a variety of substituted carbonyl chlorides, sulfonyl chorides, isocyanates, and isothiocyanates (Figure 2B, 4-A to 4-V) that were introduced by a final condensation reaction with quantitative conver-

sions. The molecules were cleaved from the resin by treatment with 50% trifluoroacetic acid in dichloromethane for 2 hr at room temperature, which typically resulted in compounds of 70%–90% purity as shown by LCMS. All compounds were further purified by HPLC using a C18 column with a 10 min gradient of 10%–95% acetonitrile/water and used as 10 mM DMSO stock solutions. Based on the initial resin loading, the overall purified yields were between 30% and 60%. This collection of analogs was screened in duplicate in the caspase activity assay.

From this small sublibrary, several derivatives were found to have significant activity, including TWX006 (IC_{50} = 10 μM) and TWX024 (IC_{50} = 25 μM) (Figure 2C). For comparison, the N7-Smac peptide inhibits the XIAP/caspase-3 interaction with an IC_{50} greater than 75 μM. Similar results were obtained using XIAP-inhibited caspase-7 (data not shown). TWX024, while slightly less potent than TWX006, exhibits higher solubility in aqueous media and was used for cellular studies.

To test whether these molecules can inhibit the function of XIAP in a more biologically relevant context, the cellular activity of TWX024 compound was examined in the 293 cell line (Figure 3). Ectopic expression of the CD95 death receptor (CD95) initiates the extrinsic apoptosis pathway, providing a death stimulus that resulted in more than 50% of transfected 293 cells undergoing apoptosis after 24 hr. Apoptotic 293 cells are detected by morphological features such as cells rounding up, detachment, and production of apoptotic bodies (Figure 3B). Coexpression of XIAP with CD95 has previously been shown to block apoptosis [10]. Consistent with this report, cotransfection of XIAP with CD95 led to survival in 95% of the transfected cells (Figure 3C), indicating that XIAP is blocking apoptosis by inhibiting caspase-3. The addition of TWX024 to 293 cells cotransfected with XIAP and CD95 significantly reversed this phenomenon and restored CD95-induced apoptosis—over 50% of the transfected cells underwent apoptosis in the presence of 25 μM TWX024 (Figure 3D). Treatment with 40 μM of TWX024 alone did not induce apoptosis (Figure 3E). These transient transfection assays provide direct evidence that TWX024 retains its ability to relieve the inhibition of XIAP on caspase-3 in cells.

TWX024 Disrupts the XIAP/Caspase-3 Interaction

A series of coprecipitation experiments were performed to confirm the ability of TWX analogs to disrupt the interaction between XIAP and active caspase-3 (Figure 4). Recombinant GST-tagged BIR1-2 was used to "pull down" caspase-3, and the complex was captured with GST-coated sepharose resins. Caspase-3 itself was not pulled down by GST-sepharose because it lacks affinity for the resins. After a series of washing to remove any nonspecifically bound proteins, the proteins retained by the resins were separated on SDS-PAGE. The presence of caspase-3 was revealed by Western blot analysis using polyclonal anti-caspase-3 antibody. When 25 μM of TWX024 was coincubated with GST-BIR1-2 and caspase-3 in PBS buffer, no caspase-3 was retained by the resins as shown by Western blot. However, 25 μM of the inactive compound TWX041 (which has no detectable activity at 100 μm concentration) did not block association of BIR1-2 and caspase-3 in these assays. These results indicate that TWX024 specifically disrupts the binding of XIAP to caspase-3.

TWX Synergizes with an Agonistic Anti-DR5 Antibody in HCT116 $Bax^{-/-}$ Cells

The induction of apoptosis through the tumor-specific TRAIL death receptor (extrinsic) pathway is a promising approach for cancer therapy [20]. Similar to CD95, TRAIL initiates apoptosis through the death receptor pathway by activating caspase-8 and then caspase-3. However, recent evidence reveals that TRAIL-mediated apoptosis is dependent upon the proapoptotic Bcl-2 family member Bax, which lies on the mitochondria (intrinsic) pathway [21, 22]. Upon stimulation by TRAIL, caspase-8 activates not only caspase-3 but also Bid, which subsequently activates Bax on the outer mitochondria membrane. Bax promotes the release of Smac, which binds to XIAP, thereby relieving the inhibition of caspase-9 and caspase-3. Without functional Bax, caspase-3 is inhibited by XIAP, resulting in reduced apoptosis even in the presence of death receptor stimulation. This cross-signaling between the two pathways is thought to be an amplification mechanism evolved to enhance the apoptosis signal initiated by the death receptor. However, in a number of human tumors (e.g., tumors exhibiting DNA mismatch repair [MMR] deficiencies) Bax is often the target of mutation and inactivation, rendering these cells TRAIL resistant [22].

Here, we ask if the TWX024 XIAP inhibitor could restore TRAIL sensitivity in a Bax-deficient HCT116 cell line [21]. HCT116 $Bax^{+/-}$ and $Bax^{-/-}$ cell lines were treated with agonistic anti-DR5 antibodies, which mimic the effect of the TRAIL ligand and selectively activate the TRAIL-DR5 receptor (our unpublished data). Consistent with the reported data, $Bax^{-/-}$ cells were significantly less sensitive to treatment with this death stimulus (80% cell viability) in contrast to $Bax^{+/-}$ cells (30% cell viability) (Figure 5). However, cotreatment with anti-DR5 and 10 μM of TWX024, but not TWX041, caused a synergistic cell death effect (50% cell viability) in Bax-deficient HCT116 cells. Hence, these data strongly suggest that TWX024 substituted for the function of endogenous Smac by inhibiting the XIAP/caspase-3 interaction, thereby facilitating caspase activation and apoptosis. Interestingly, treatment with TWX024 alone did not cause elevated death in HCT116 cells. It is possible that without a proapoptotic signal, simply removing the XIAP inhibition on caspase-3 does not trigger significant apoptosis because most caspase-3 exists in the inactive procaspase form. Therefore, unless there is an apoptosis signal to mature procaspase-3, relief of XIAP inhibition alone does not promote apoptosis. Taken together, the synergistic effect of TRAIL-DR5 agonists and TWX024 can be extended to cells having other proapoptotic defects in the mitochondrial release of Smac.

Structural-Activity Relationship and Modeling

An analysis of the structure-activity relationship (SAR) data generated from screening the focused library pro-

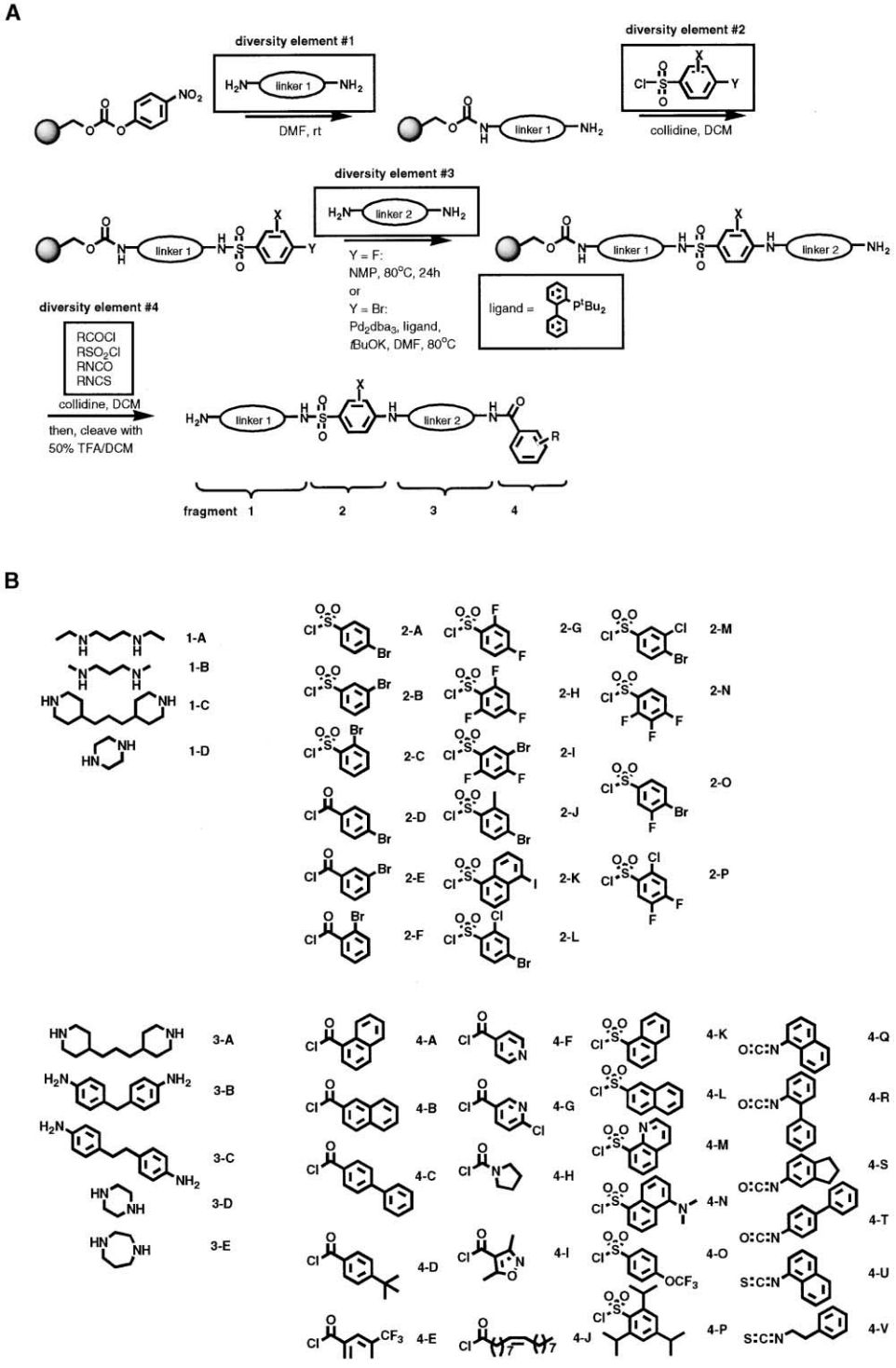

Figure 2. Continued on next page.

vided insights into the structural features necessary for inhibitor activity (Figure 2C). The flexible acyclic diamines had higher activity than cyclic diamines when substituted in fragment one. Ethyl substituents on either nitrogen led to increased activity relative to methyl substitution (propyl or larger substituents were not tested), indicating that hydrophobicity is critical for activity. Aryl sulfonyl groups had increased activity relative to carbonyl groups when substituted in the second fragment—molecules derived from the aryl acid chlorides 2-D and 2-E have essentially no activity relative to those containing the aryl sulfonamide 2-A and 2-B, suggesting that proper positioning of the H bond donor oxygen is critical for binding. The second and third fragments can

C

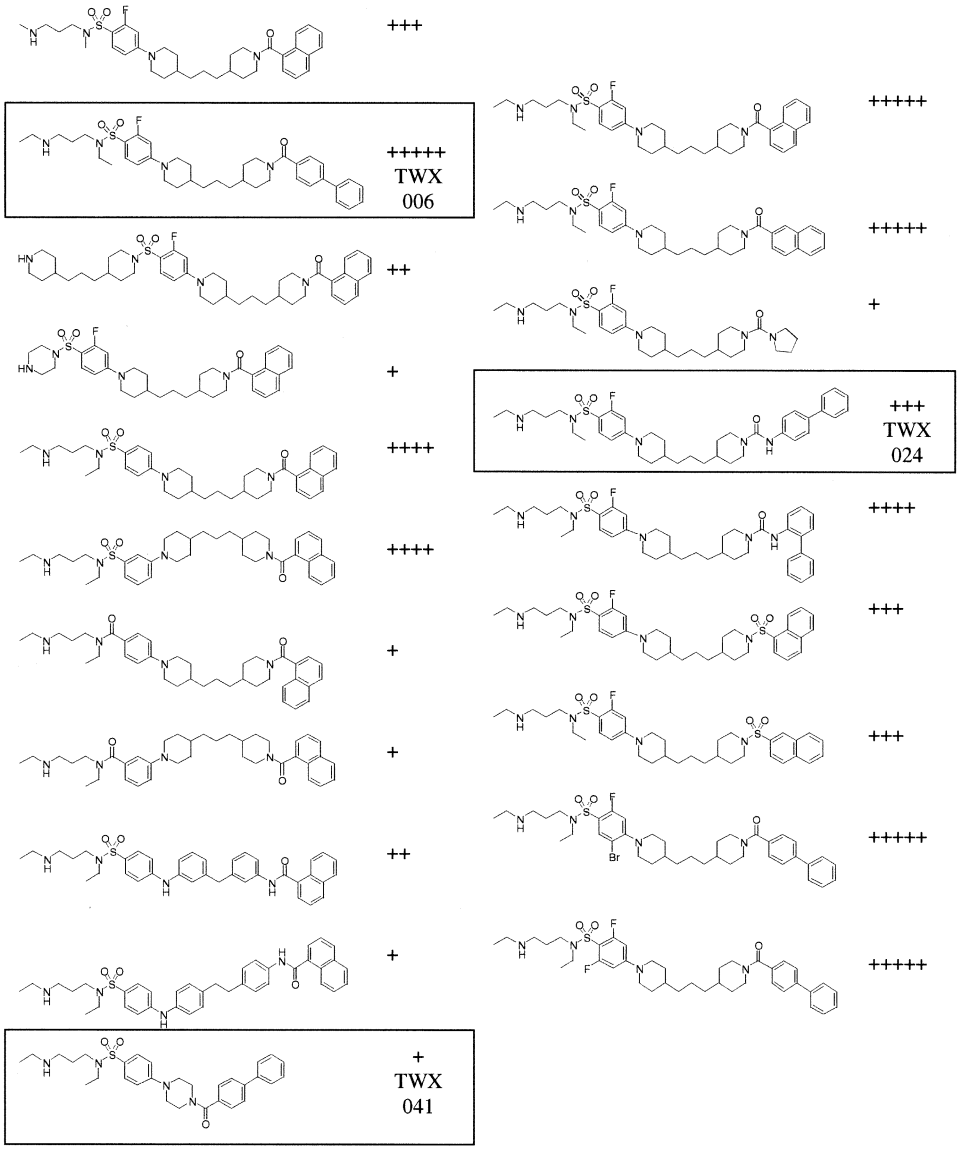

Figure 2. Chemical Synthesis of TWX Analogs

(A) Synthetic scheme for TWX analogs.

(B) Diversity elements used in the synthesis of TWX analogs.

(C) Structures and activities of selected TWX analogs. Plus marks (+) represent the percentage of XIAP inhibition at 20 μM of small molecule: +++++, 80%–100%; ++++, 60%–79%; +++, 40%–59%; ++, 20%–39%; +, 0%–19%. These compounds do not affect caspase-3 activity in the absence of XIAP.

be *para* or *meta* linked, but *ortho* linkage (2-C) decreases activity dramatically. Addition of an ortho-fluorine atom on the aromatic ring of fragment two increases activity; 2-G was the optimal second fragment examined. The more rigid fragments (3-B and 3-C) and shorter fragments (3-D and 3-E) both have considerably lower activity than 3-A. The scaffold can tolerate a wide variety of large, hydrophobic groups in the fourth fragment, as 4-A to 4-D all have similar activities. Smaller, more polar groups result in lower activities, which implies fragment four occupies a large hydrophobic pocket. A long aliphatic chain (4-J) also has poor activity. The ureido group (4-Q) improved the solubility of the molecule (e.g., TWX024), although amide (4-C) serves as the best linkage between the third and fourth fragment. Attempts to make truncated versions in which N- or C-terminal fragments were deleted resulted in a loss of activity.

This SAR data was used together with molecular models of the interaction between TWX006 and XIAP to begin to gain insights into how TWX006 might inhibit the interaction of XIAP with caspase-3. Initially, the optimal binding site for TWX006 was searched on available XIAP

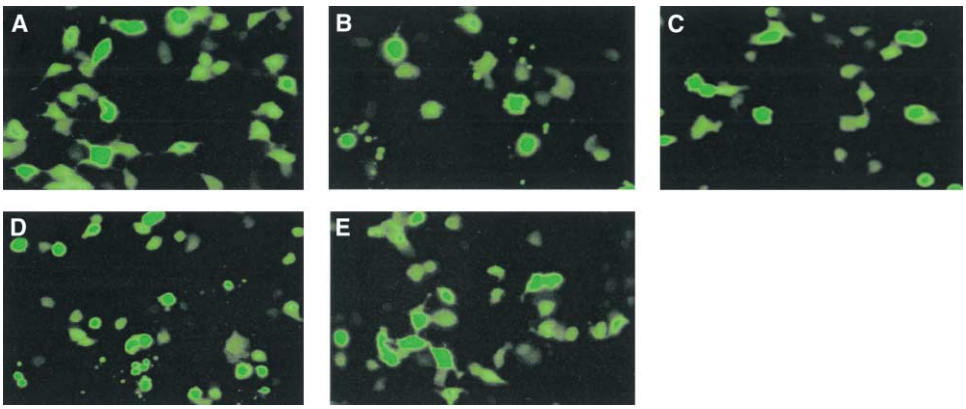

Figure 3. 293 Cell Transfection Assays

(A) Cells transfected with GFP as a positive control exhibit normal cell morphology.

(B) Over 50% of cells transfected with pcDNA3-CD95 underwent apoptosis, as indicated by the production of apoptotic bodies.

(C) Transfection of pcDNA3-XIAP along with pcDNA3-CD95 blocked apoptosis in 95% of transfected cells.

(D) Addition of TWX024 (25 μM) to cells transfected with pcDNA3-CD95 and pcDNA3-XIAP induced apoptosis in up to 50% of transfected cells.

(E) Treatment with TWX024 (40 μM) alone has no apoptosis-inducing effect.

and caspase-3 structures (1I3O.pdb) using Glide (version 2.0). Once confined to a specific binding surface, the small molecule binding conformation was optimized using a mixed Monte Carlo Mulitple Minimum (MCMM) algorithm provided by MacroModel (version 7.0). The resultant model predicts that TWX006 occupies the linker region between BIR1 and BIR2 of XIAP (Figure 6); the same region caspase-3 was shown to bind in the previous crystallographic studies [7–9]. The key features of this model are supported by the SAR generated from the focused library of TWX analogs.

The modeling experiments suggest that the terminal-amino group of fragment 1-A forms H bonds with the sidechains of Asp 214 and Glu 219 of BIR2, and the sulfonyl oxygen of element 2-G makes a H bond with the backbone nitrogen of Lys 208 of BIR2. Switching the sulfonyl to a carbonyl for fragment two (2-D)

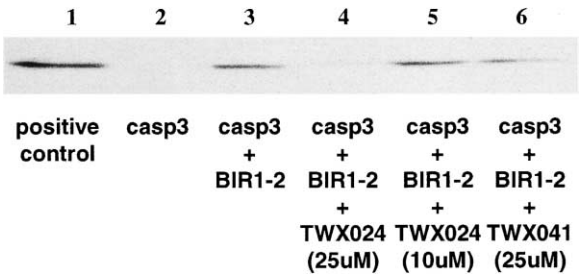

Figure 4. GST-BIR1-2 Coprecipitation Experiments

SDS-PAGE followed by caspase-3 Western blot was performed with the proteins retained by GST-sepharose resins. Recombinant active caspase-3 was loaded as a positive control (lane 1). Active caspase-3 lacking a GST tag was not retained by GST-sepharose (lane 2). However, coincubation of caspase-3 along with GST-BIR1-2 resulted in the coprecipitation of caspase-3 (lane 3). Addition of TWX024 at 25 μM prevented/disrupted the binding of GST-BIR1-2 to caspase-3 (lane 4). Lower concentrations of TWX024 (10 μM) or TWX041 (25 μM) did not affect the binding of caspase-3 to GST-BIR1-2 (lanes 5 and 6).

lowers the binding affinity possibly by disrupting the optimal H bond angle. In the docked complex, TWX006 twists through a hydrophobic groove of BIR2. A long and flexible dipiperidine moiety (3-A) is necessary to avoid a steric clash with a side chain protruding into the groove, again consistent with the SAR data. The model places the fourth fragment of the inhibitor into the hydrophobic site occupied by residues of caspase-3 in the corresponding caspase-3/XIAP complex. It is likely that fragment 4-C interferes with caspases-3 binding by occupying the binding surface composed of residues Ser 150, Tyr 154, Cys 203, and Phe 228 of BIR2. In the BIR2/caspase-3 complex, this hydrophobic region is occupied by caspase-3 residue Met 316, whose backbone oxygen H bonds to the backbone nitrogen of Asn 226 of BIR2. In the TWX006/caspase-3 complex the backbone nitrogen of Asn 226 of BIR2 is H bonded with carbonyl oxygen of fragment 4-C. The experimental observation that a bulkier fourth diversity element has higher activity is consistent with the proposed binding model of TWX006, as it predicts better interactions with the hydrophobic region at the caspases-3 binding site. The flexibility and length of the third diversity element is also critical, since the model suggests that rigid and/or shorter moieties will reduce the extension of the molecule into the caspase-3 binding region. TWX041 does not have the length required for extension into the caspases-3 binding interface and therefore has reduced activity. The observation that TWX also relieves BIR2 inhibition on caspase-7 suggests that the same mechanism of protein complex disruption can also be implied with XIAP/caspase-7 given the structural similarity of caspase-3 and -7.

Based on the predicted TWX binding model and SAR data, active TWX analogs disrupt the XIAP/caspase-3 complex by directly occupying the protein-protein interaction interface (the linker region between BIR1 and BIR2). Full-length Smac protein, an endogenously expressed inhibitor of the XIAP/caspase-3 interaction, binds to BIR2 and extends itself into the linker region,

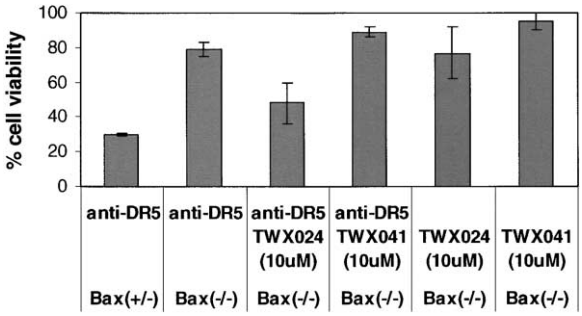

Figure 5. TWX Synergy with Agonistic Antibodies Specific for the TRAIL Death Receptor DR5

HCT116 $Bax^{+/-}$ and HCT $Bax^{-/-}$ cells were treated with anti-DR5 with or without 10 μM TWX. $Bax^{+/-}$ cells were sensitive to anti-DR5 treatment, but $Bax^{-/-}$ cells were not. Addition of TWX024, but not TWX041, sensitized $Bax^{-/-}$ cells to the proapoptotic effect of anti-DR5. As a control, TWX024 alone has relatively low toxicity in $HCT116^{-/-}$ cells.

thereby preventing the binding of caspase-3 through a buttress effect [9]. Although N7-Smac peptide may have binding affinity for BIR2, it lacks the sterical bulkiness required to hinder binding of caspase-3 to the linker region. The inhibition of caspase-9 by XIAP operates through a different mechanism [14], which implies that the Smac-mediated relief of caspase-9 inhibition must also be different than that of caspase-3. Smac protein displaces XIAP from caspase-9 by directly competing for the BIR3 domain [12, 13]. Hence, N-terminal Smac peptide and derivatives retain the XIAP inhibitory activity on caspase-9 because of their high affinity for the BIR3 domain [10], but cannot also disrupt the XIAP/caspase-3 interaction. This suggests that compounds such as TWX006 or TWX024, which bind directly to the linker region between BIR1 and BIR2, are better than Smac peptidomimetics for developing small molecule drugs that target the XIAP/caspase-3 interaction.

Significance

High-throughput screening and parallel solid-phase organic synthesis were used to rapidly identify a series of small molecule inhibitors of the caspase-3/XIAP interaction. The TWX compounds represent the first generation of small molecules capable of interfering with XIAP's ability to inhibit executioner caspases-3 and -7. These compounds were employed to probe XIAP function in tumor cells lines and to show that they could be used to "bypass" the apoptosis block resulting from the loss of the proapoptotic Bcl-2 family member Bax in a colon carcinoma cell line. Since many tumor cells evade apoptosis by dampening the intrinsic mitochondrial apoptosis pathway, these compounds will be useful for further elucidation of these tumor cell survival strategies and may facilitate development of therapeutically useful agents that target XIAP function in relevant carcinomas.

Experimental Procedures

High-Throughput Screening and Caspase Activity Assays

Caspase activities were assayed as previously described [23] at 37°C in 6 μl caspase buffer (50 mM HEPES, pH 7.4, 100 mM NaCl, 10% sucrose, 1 mM EDTA, 0.1% CHAPS). The high-throughput screens were carried out in 1536-well formats. Recombinant XIAP-BIR2 (5 μl, 21.3 nM) in caspase buffer (with 296 μM Ac-DEVD-afc; Calbiochem, San Diego, CA) was added to the wells, followed by addition of compound in neat DMSO (final compound concentration about 10 μM). The mixture was incubated at room temperature for 20 min. Caspase-3 (1 μl, 12.5 nM) in caspase buffer (with 10 mM DTT) was added to each well. An initial fluorescence reading (Acquest LJL Biosystems, Molecular Device Corporation, Sunnyvale, CA) was measured followed by a final reading after 1 hr incubation. Activity was measured as the difference in signal between the final read

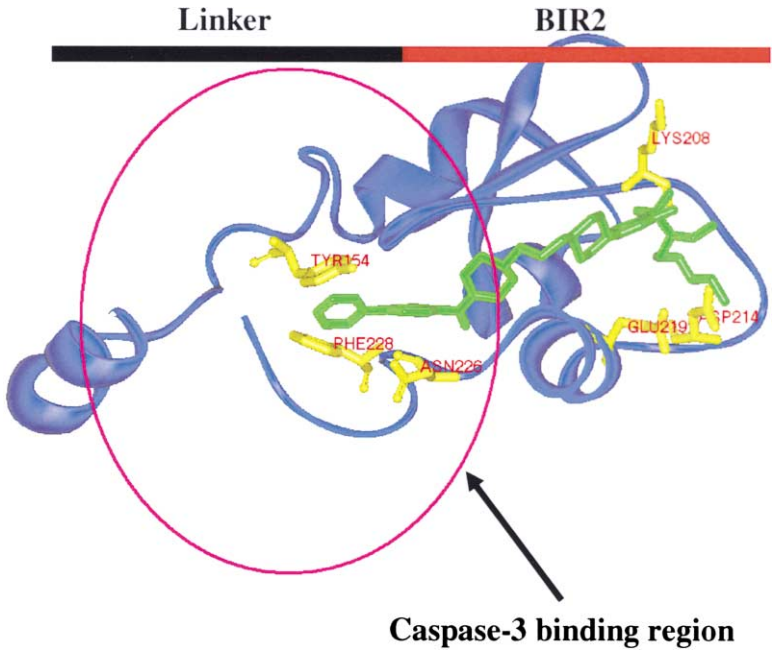

Figure 6. Computational Modeling of TWX Binding to XIAP

A computational model of TWX binding to XIAP-BIR2. The TWX binding surface shares a significant overlap with the caspase-3 binding surface. TWX006 (green) makes critical H bond contacts with Asp 214, Glu 219, and Lys 208 of BIR2. The fourth fragment of TWX006 occupies the hydrophobic pocket formed by Asn 226, Tyr 154, and Phe 228 of BIR2, extending into the caspase-3 binding region.

and the initial read. Postscreening IC_{50} tests on selected compounds were carried out in 384-well formats in 40 μl caspase buffer using a continuous reading fluorometer (Molecular Devices Spectramax, Molecular Device). The assay procedure was the same except that fluorescence measurements were taken in the kinetic mode.

Chemistry

All reagents and solvents were purchased from Sigma/Aldrich (Milwaukee, WI); the palladium catalysts and ligands were purchased from Strem Chemicals (Newburyport, MA). Carbamate resin was made in bulk quantity according to reported literature [18]. For each TWX analog, 100–500 mg of carbamate resin (0.8 mmol/g) was mixed with the first diversity element (20 equivalents [eq.]) dissolved in *N,N*-dimethylformamide (DMF) and shaken at room temperature overnight. The resins were then washed successively with dichloromethane (DCM) and DMF for four times and dried under vacuum overnight. Subsequently, the resins were suspended in DCM and treated with the second diversity element (5 eq.), collidine (5 eq.), and shaken at room temperature overnight, followed by washing and drying. For X = F, the third diversity element (20 eq.) was heated with the resins in *N*-methylpyrrolidine at 80°C for 24 hr. For X = Br or I, the third diversity element (10 eq.) was mixed with the resins along with Pd_2dba_3 (0.15 eq.), ligand (0.6 eq.), potassium *tert*-butoxide (10 eq.), and DMF and heated to 80°C under argon atmosphere for 18 hr. After washing and drying, the resins were suspended in DCM and treated with the fourth diversity element (5 eq.), collidine (5 eq.), and shaken at room temperature overnight. The resins were wash and dried. Cleavage is mediated by treatment of the resin with a cocktail of TFA/DCM/Me_2S/H_2O (45:45:5:5) for 2 hr at room temperature. The liquid was drained and the resins were washed one time with DCM. The combined liquid was concentrated and subjected to HPLC using a C18 reverse column and eluting with 5%–95% acetonitrile in water gradient. The purified compounds were concentrated and typical yields are between 30% and 60% relative to initial resin loading. All compound were dissolved as 10 mM stock solution for assays. Purity of compounds was assessed by reverse-phase liquid chromatography mass spectrometry (4 min elution using 5%–95% acetonitrile in water) with an UV detector at λ = 255 nm and an electrospray ionization source. TWX006: $C_{39}H_{53}FN_4O_3S$ calc'd 676.4, found [MH^+] 677.4; TWX024: $C_{39}H_{54}FN_5O_3S$ calc'd 691.4, found [MH^+] 692.4; TWX041 $C_{30}H_{37}FN_4O_3S$ calc'd 552.3, found [MH^+] 553.3.

TWX024: ^{1}H NMR (500 MHz, $CDCl_3$) δ 8.68 (br, 2H), 7.39–7.49 (m, 5H), 7.28–7.31 (m, 3H), 7.18 (t, J = 7.8 Hz, 1H), 6.97 (s, 1H), 6.45 (d, J = 9.1 Hz, 1H), 6.37 (d, J = 14.7 Hz, 1H), 3.96 (d, J = 12.9, 2H), 3.65 (d, J = 12.6, 2H), 3.33 (s, 1H), 3.18 (m, 2H), 3.07 (q, J = 7.1 Hz, 2H), 2.86–2.93 (m, 4H), 2.73 (t, J = 12.4 Hz, 4H), 1.82 (m, 2H), 1.62 (t, J = 14.3 Hz, 4H), 1.32 (m, 2H), 0.99–1.20 (m, 12H), 0.92 (t, J = 7.2 Hz, 3H). ^{13}C NMR (500 MHz, $CDCl_3$) δ 161.6, 159.1, 155.6, 140.7, 138.9, 135.7, 132.0, 128.8, 127.4, 126.8, 120.7, 113.4, 113.2, 108.9, 101.2, 47.8, 44.8, 44.35, 44.32, 43.3, 43.0, 36.6, 36.5, 35.9, 35.6, 32.2, 31.6, 25.4, 23.6, 13.7, 11.2.

Proteins Expression and Purification

The GST fusion proteins XIAP-BIR1-2 and XIAP-BIR3-RING were prepared as previously described from the soluble fraction upon induction with 0.4 mM IPTG at 30°C for 3–20 hr and then purified by glutathione-sepharose affinity chromatography [6]. Recombinant caspase-3 was a kind gift from G. Salvesen (The Burnham Institute, San Diego, CA).

Cell Culture, Transfection, and Cytotoxicity Assays

293 cells were cultured in Dulbecco's modified Eagles medium (DMEM) supplemented with 10% fetal bovine serum (FBS). One day before transfection, the 293 cells were split and plated in 12-well tissue culture plates, each well containing 1 ml of cells at 8×10^4 cells/ml. Transfections were carried out with a Fugene to DNA ratio of 3 μl to 1.2 μg DNA with the following DNA concentrations: 0.2 μg of the green fluorescent protein (GFP) marker plasmid pEGFP (Clontech), 0.2 μg pCMV-Fas, and 0.8 μg pcDNA3-XIAP or the control plasmid pcDNA3 empty. The reactions were incubated at room temperature for 30 min and then added to the cells. After 4 hr of incubation at 37°C, the media was removed and 1 ml of fresh DMEM (with 10% FBS) was added. Compounds were also added at this time. Cells were imaged with a fluorescence microscope 24 hr after addition of the compounds. HCT116 $Bax^{+/-}$ and $Bax^{-/-}$ cells were cultured in RPMI supplemented with 10% FBS. One day before addition of anti-DR5 and TWX compound, cells were split and plated in 96-well tissue culture plates, each containing 100 μl of cells at 1×10^5 cells/ml. Anti-DR5 (2 μg/μl) and compounds were added to the wells as described in Figure 5. The MTT assay, which is a colorimetric assay based on the ability of viable cells to reduce a soluble yellow tetrazolium salt (MTT) to blue formazan crystals, was used to determine the number of viable cells.

Pull-Down Assay and Western Blot Analysis

Glutathione-sepharose resins (20 μl) were incubated with caspase-3 (1 nM), XIAP-BIR1-2 or XIAP-BIR3-RING (50 nM), and TWX (in accordance with Figure 3) in 60 μl PBS at 4°C for 30 min. The samples were centrifuged at 1000 rpm for 5 min. The supernatant was removed and the beads were washed three times with 100 μl PBS. SDS sample loading buffer (20 μl) was added to the beads and heated at 95°C for 5 min. Each sample was subsequently separated under reducing conditions on 10%–20% gradient SDS-polyacrylamide gels. After transfer to nitrocellulose membranes, the membranes were incubated for 1 hr in 10% nonfat milk powder followed by 1 hr incubation with the rabbit anti-caspase3 polyclonal antibody (1:1000; Pharmingen, San Diego, CA). The membrane was washed fives times with PBS/0.05% Tween, incubated with anti-rabbit peroxidase-conjugated affinity-purified secondary antibody (1:5000; Biorad, Hercules, CA) for 30 min, washed again five times, developed using enhanced chemiluminescence (ECL; Amersham, Piscataway, NJ), and exposed to Kodak Biomax films.

Virtual Modeling

The virtual model was constructed using two computational softwares (Glide and MacroModel) and based on the published crystal structure of XIAP/caspase-3 that can be downloaded from the Protein Data Bank (1I3O.pdb). Flexible ligand docking was performed with Glide (version 2.0; Schrodinger Inc., Portland, OR). For the grids calculation, the van der Waals radii of nonpolar protein atoms were scaled by a factor of 0.9. The enclosing box for ligand docking was centered on the Smac binding pocket and was 34 Å in size along each dimension. Electrostatic interactions were calculated with a distance-dependent dielectric constant 2r. The van der Waals radii of nonpolar ligand atoms were scaled by a factor of 0.8. The maximum number of poses selected for refinement was 5000, and the maximum number of refined poses selected final minimization and scoring was set at 400. Flexible protein/ligand docking was performed using the mixed Monte Carlo Multiple Minimum (MCMM)/LLMOD (Large Scale LowMode) conformational search strategy available in MacroModel (version 7.0; Schrodinger Inc.). During the LLMOD structural perturbation and subsequent minimization, seven protein residues were allowed to move freely: Tyr 154, Leu 207, Trp 210, His 223, Phe 224, Asn 226, and Phe 228. The remaining residues were not allowed to move; however, their electrostatic and van der Waals interactions with moving atoms was included in the calculation. The inhibitor TWX006 was allowed to move freely during the LLMOD step and subsequent minimization. In order to initiate the MCMM/LLMOD search the TWX006 inhibitor was placed into the receptor in the orientation/conformation derived from the docking by Glide. A 20,000 step search was conducted, which required 148,500 CPU seconds on a single XEON processor. A 30 kJ/mol window contained 130 unique structures and the global energy minimum was found 33 times during the conformational search. The rmsd value between heavy atoms of freely moving residues of initial and global minimum conformations was 0.49 Å.

Acknowledgments

We thank M. Marlowe and J. Caldwell (GNF, San Diego, CA) for high-throughput screening, J. Graziano (TSRI, La Jolla, CA) for recombinant XIAP, G. Salvesen (The Burnham Insitute, San Diego, CA) for recombinant caspase-3, B. Vogelstein (John Hopkins University, Baltimore, MD) for HCT116 cell lines, M. Nasoff (GNF) for anti-DR5

antibodies, N.S. Gray (GNF) for discussion and support, and Novartis Research Foundation for support.

Received: April 9, 2003
Revised: June 12, 2003
Accepted: June 26, 2003
Published: August 22, 2003

References

1. Hanahan, D., and Weinberg, R.A. (2000). The hallmarks of cancer. Cell *100*, 57–70.
2. Huang, Z. (2002). The chemical biology of apoptosis: exploring protein-protein interactions and the life and death of cells with small molecules. Chem. Biol. *9*, 1059–1072.
3. Salvesen, G.S., and Duckett, C.S. (2002). IAP proteins: blocking the road to death's door. Nat. Rev. Mol. Cell Biol. *3*, 401–410.
4. Holcik, M., and Korneluk, R.G. (2001). XIAP, the guardian angel. Nat. Rev. Mol. Cell Biol. *2*, 550–556.
5. Morris, M.J., Tong, W.P., Cordon-Cardo, C., Drobnjak, M., Kelly, W.K., Slovin, S.F., Terry, K.L., Siedlecki, K., Swanson, P., Rafi, M., et al. (2002). Phase I trial of BCL-2 antisense oligonucleotide (G3139) administered by continuous intravenous infusion in patients with advanced cancer. Clin. Cancer Res. *8*, 679–683.
6. Deveraux, Q.L., Takahashi, R., Salvesen, G.S., and Reed, J.C. (1997). X-linked IAP is a direct inhibitor of cell-death proteases. Nature *388*, 300–304.
7. Chai, J., Shiozaki, E., Srinivasula, S.M., Wu, Q., Dataa, P., Alnemri, E.S., and Shi, Y. (2001). Structural basis of caspase-7 inhibition by XIAP. Cell *104*, 769–780.
8. Huang, Y., Park, Y.C., Rich, R.L., Segal, D., Myszka, D.G., and Wu, H. (2001). Structural basis of caspase inhibition by XIAP: differential roles of the linker versus the BIR domain. Cell *104*, 781–790.
9. Riedl, S.J., Renatus, M., Schwarzenbacher, R., Zhou, Q., Sun, C., Fesik, S.W., Liddington, R.C., and Salvesen, G.S. (2001). Structural basis for the inhibition of caspase-3 by XIAP. Cell *104*, 791–800.
10. Deveraux, Q.L., Leo, E., Stennicke, H.R., Welsh, K., Salvesen, G.S., and Reed, J.C. (1999). Cleavage of human inhibitor of apoptosis protein XIAP results in fragments with distinct specificities for caspases. EMBO J. *18*, 5242–5251.
11. Du, C., Fang, M., Li, Y., Li, L., and Wang, X. (2000). Smac, a mitochondrial protein that promotes cytochrome c-dependent caspase activation by eliminating IAP inhibition. Cell *102*, 33–42.
12. Liu, Z., Sun, C., Olejniczak, E.T., Meadows, R.P., Betz, S.F., Oost, T., Herrmann, J., Wu, J.C., and Fesik, S.W. (2001). Structural basis for binding of Smac/DIABLO to the XIAP BIR3 domain. Nature *408*, 1004–1008.
13. Wu, G., Chai, J., Suber, T.L., Wu, J.-W., Du, C., Wang, X., and Shi, Y. (2001). Structural basis of IAP recognition by Smac/DIABLO. Nature *408*, 1008–1012.
14. Shiozaki, E.N., Chai, J., Rigotti, D.J., Riedl, S.J., Li, P., Srinivasula, S.M., Alnemri, E.S., Fairman, R., and Shi, Y. (2003). Mechanism of XIAP-mediated inhibition of caspase-9. Mol. Cell *11*, 519–527.
15. Kipp, R.A., Case, M.A., Wist, A.D., Cresson, C.M., Carrell, M., Griner, E., Wiita, A., Albiniak, P.A., Chai, J., Shi, Y., et al. (2002). Molecular targeting of inhibitor of apoptosis proteins based on small molecule mimics of natural binding partners. Biochemistry *41*, 7344–7349.
16. Chia, J., Du, C., Wu, J.-W., Kyin, S., Wang, X., and Shi, Y. (2000). Structural and biochemical basis of apoptotic activation by Smac/DIABLO. Nature *406*, 855–862.
17. Deveraux, Q.L., Welsh, K., and Reed, J.C. (2000). Purification and use of recombinant inhibitor of apoptosis proteins as caspase inhibitors. Methods Enzymol. *322*, 154–161.
18. Smith, A.L., Stevenson, G.I., Lewis, S., Patel, S., and Castro, J.L. (2000). Solid-phase synthesis of 2,3-disubstituted indoles: discovery of a novel, high-affinity h5-HT_{2A} antagonist. Bioorg. Med. Chem. Lett. *10*, 2693–2696.
19. Wolfe, J.P., Tomori, H., Sadighi, J.P., Yin, J., and Buchwald, S.L. (2000). Simple, efficient catalyst system for the palladium-catalyzed amination of aryl chlorides, bromides, and triflates. J. Org. Chem. *65*, 1144–1157.
20. Wajant, H., Pfizenmaier, K., and Scheurich, P. (2002). TNF-related apoptosis inducing ligand (TRAIL) and its receptors in tumor surveillance and cancer therapy. Apoptosis *7*, 449–459.
21. Deng, Y., Lin, Y., and Wu, X. (2002). TRIAL-induced apoptosis requires Bax-dependent mitochondrial release of Smac/DIABLO. Genes Dev. *16*, 33–45.
22. LeBlanc, H., Lawrence, D., Varfolomeev, E., Totpal, K., Morlan, J., Schow, P., Fong, S., Schwall, R., Sinicropi, D., and Ashkenazi, A. (2002). Tumor-cell resistance to death receptor-induced apoptosis through mutational inactivation of the proapoptotic Bcl-2 homolog bax. Nat. Med. *8*, 274–281.
23. Stenicke, H.R., and Salvesen, G.S. (2000). Caspase assays. Methods Enzymol. *332*, 91–100.